

# Higher Twist Analysis of the Proton $g_1$ Structure Function

M. Osipenko<sup>1</sup>, W. Melnitchouk<sup>2</sup>, S. Simula<sup>3</sup>, P. Bosted<sup>4</sup>, V. Burkert<sup>2</sup>,

M. E. Christy<sup>5</sup>, K. Grioren<sup>6</sup>, C. Keppel<sup>2;5</sup>, S. E. Kuhn<sup>7</sup>

<sup>1</sup> INFN, Sezione di Genova, 16146, Genoa, Italy

<sup>2</sup> Jefferson Lab, 12000 Jefferson Avenue, Newport News, Virginia 23606, USA

<sup>3</sup> INFN, Sezione Roma III, 00146 Roma, Italy

<sup>4</sup> University of Massachusetts, Amherst, Massachusetts 01003, USA

<sup>5</sup> Hampton University, Hampton, Virginia 23668, USA

<sup>6</sup> College of William & Mary, Williamsburg, Virginia, 23187, USA

<sup>7</sup> Old Dominion University, Norfolk, Virginia 23529, USA

We perform a global analysis of all available spin-dependent proton structure function data, covering a large range of  $Q^2$ ,  $1 < Q^2 < 30 \text{ GeV}^2$ , and calculate the lowest moment of the  $g_1$  structure function as a function of  $Q^2$ . The moment at high  $Q^2$  is used to obtain a value of the singlet axial charge, consistent with all the proton data. From the  $Q^2$  dependence of the lowest moment we extract matrix elements of twist-4 operators, and determine the color electric and magnetic polarizabilities of the proton.

PACS numbers: 12.38Aw, 12.38Qk, 13.60Hb

Measurements of spin-dependent structure functions of the proton reveal fundamental information about the proton's quark and gluon structure. In the quark-parton model, the  $g_1$  structure function is interpreted in terms of distributions of quarks carrying light-cone momentum fraction  $x$ , with spins aligned versus anti-aligned with that of the nucleon. The lowest moment, or integral over  $x$ , of the  $g_1$  structure function also determines the total spin carried by quarks in the nucleon.

While most structure function studies have focused on the scaling regime at high four-momentum transfer squared,  $Q^2$ , the behavior of the  $g_1$  structure function and its moments in the transition region at intermediate  $Q^2$  ( $\sim 1 \text{ GeV}^2$ ) can reveal rich information about the long-distance structure of the nucleon. One example of the complexity of this region is the transition from the Bjorken or Ellis-Jae sum rules at high  $Q^2$  to the Gerasimov-Drell-Hearn sum rule at  $Q^2 = 0$  [1].

Of particular importance in the intermediate  $Q^2$  region is the role of the nucleon resonances, and the related phenomenon of quark-hadron duality. At  $Q^2 \sim 1 \text{ GeV}^2$  much of the strength of the structure function moment comes from the resonance region, in which the mass of the hadronic final state  $W < 2 \text{ GeV}$  (see Fig. 1 below). Recent results from Jefferson Lab on the spin-averaged structure function of the proton [2] suggest remarkable agreement between the scaling function measured at high  $Q^2$ , and the averaged resonance contributions at low  $Q^2$  and  $W$ .

According to the operator product expansion (OPE) in QCD, the appearance of the resonance (scaling duality is related to the size of higher twist corrections to moments of the structure functions [3]). Higher twists are expressed as matrix elements of operators involving nonperturbative interactions between quarks and gluons. Dominance of the leading twist (scaling) contribution, which corre-

sponds to incoherent scattering from individual quarks, would lead to duality. Conversely, violations of duality signal the presence of higher twist corrections, and the importance of long distance quark-gluon correlations.

In this paper we determine the size of the higher twist contributions to the lowest moment of the  $g_1$  structure function of the proton. We analyze the entire set of available data from experiments at SLAC [4, 5, 6, 7], CERN [8, 9], DESY [10], and most recently Jefferson Lab [11], where high-precision data in the resonance region and at low and intermediate  $Q^2$  have been taken. Earlier studies [12, 13] have only considered subsets of the data now available, covering considerably smaller regions of kinematics. Combining the new Jefferson Lab results with the earlier data is nontrivial, however, since the various analyses typically make use of different assumptions about extrapolations into unmeasured regions of kinematics. In the present analysis, we therefore extract the structure function moment using a single, consistent set of inputs and assumptions.

The lowest (Comwall-Norton) moment of the  $g_1$  structure function of the proton is defined as

$$\Gamma_1(Q^2) = \int_0^1 dx g_1(x; Q^2); \quad (1)$$

where the upper limit includes the proton elastic contribution at  $x = Q^2 = 2M^2 = 1$ , where  $\nu$  is the energy transfer, and  $M$  is the proton mass. The inclusion of the elastic component is essential if one wishes to use the OPE to study the evolution of the integral in the moderate  $Q^2$  region [14].

From the OPE, in the limit of large  $Q^2$   $\gg \Lambda_{\text{QCD}}^2$  the moment  $\Gamma_1$  can be expanded in powers of  $1/Q^2$ , with the expansion coefficients related to nucleon matrix elements of operators of a definite twist (defined as the dimension minus the spin of the operator). At high  $Q^2$  the moment

is dominated by the leading (twist-2) contribution,  $f_2$ , which is given in terms of matrix elements of the axial vector current,  $J_5$ . This can be decomposed into singlet and nonsinglet contributions as

$$f_2(Q^2) = C_s(Q^2) \frac{a_0^{\text{inv}}}{9} + C_{\text{ns}}(Q^2) \frac{a_3}{12} + \frac{a_8}{36} \quad (2)$$

where  $C_s$  and  $C_{\text{ns}}$  are the singlet and nonsinglet Wilson coefficients, respectively [15], which are calculated as a series in  $\alpha_s$ . The triplet and octet axial charges are extracted from weak decay matrix elements,  $a_3 = g_A = 1.267$ ,  $a_8 = 0.58$ . For the singlet axial charge, we work with the renormalization group invariant definition in the  $\overline{\text{MS}}$  scheme,  $a_0^{\text{inv}} = a_0(Q^2 = 1)$ , in which all of the  $Q^2$  dependence is factorized into the Wilson coefficient  $C_s$ .

Considerable effort has been made over the past two decades in determining the singlet charge, which in the quark-parton model is identified with the total spin carried by quarks in the proton. In this work we focus instead on using the world's data to extract the coefficient of the  $1=Q^2$  subleading, twist-4 term, which contains information on quark-gluon correlations in the nucleon.

In addition to the twist-4 matrix element, the  $1=Q^2$  term also contains so-called "kinematic" higher twists, associated with target mass corrections (which are formally twist-2), and the  $g_2$  structure function, which is obtained from measurements with transversely polarized targets. One technique for removing these is to work in terms of the Nachtmann moment [16],

$$M_1(Q^2) = \int_0^1 dx \frac{x^2}{x^2} g_1(x; Q^2) \frac{x}{1-x} \frac{1-M^2x}{9Q^2} - \frac{4M^2x^2}{3Q^2} g_2(x; Q^2); \quad (3)$$

where  $\xi = 2x/(1 + \sqrt{1 + 4M^2x^2/Q^2})$  is the Nachtmann scaling variable. The twist expansion of  $M_1(Q^2)$  then yields

$$M_1(Q^2) = f_2(Q^2) + \frac{f_4(Q^2)}{Q^2} + \frac{f_6(Q^2)}{Q^4} + \dots$$

where  $f_2$  is given in Eq. (2). The  $1=Q^2$  correction in Eq. (4) exposes directly the "dynamical" twist-4 coefficient  $f_2$ ,

$$f_4(Q^2) = \frac{4M^2}{9Q^2} f_2(Q^2); \quad (5)$$

where  $f_2$  is given in terms of the matrix element of a mixed quark-gluon operator,

$$f_2(Q^2) M^2 S = \frac{1}{2} \int \frac{d^4x}{(2\pi)^4} e^{iq \cdot x} \langle N | \bar{\psi}(0) \gamma_5 \psi(x) + \bar{\psi}(0) \gamma_5 \mathcal{G}(x) \psi(x) | N \rangle; \quad (6)$$

Here  $\mathcal{G} = \frac{1}{2} G$  is the dual of the gluon field strength tensor,  $S$  is the proton spin vector,  $g$  is the strong coupling constant, and  $e_q$  is the quark charge.

Clearly the  $1=Q^2$  term can be best determined in the intermediate  $Q^2$  region, where  $Q^2$  is neither so large as to completely suppress the higher twists, nor so small as to render the twist expansion unreliable. A meaningful analysis of data from different experiments further demands that a consistent set of inputs be used in the determination of  $g_1$ , as well as  $g_2$ . In practice one must reconstruct  $g_1$  from a combination of longitudinal ( $A_k$ ) and transverse ( $A_\perp$ ) polarization asymmetries,

$$g_1(x; Q^2) = \frac{F_1(x; Q^2)}{d^0} A_k + \tan \frac{A_\perp}{2}; \quad (7)$$

together with the unpolarized  $F_1$  structure function, and the ratio  $R$  of the longitudinal to transverse cross sections, which enters through the kinematic factor  $d^0 = (1 - \cos^2 \theta) (2E - 1) = (1 + R(x; Q^2))$ , with  $\theta = (1 + 2(1 + Q^2) \tan^2 \frac{\theta}{2})^{-1/2}$ , where  $\theta$  is the lepton scattering angle. We begin by collecting all available data on  $A_k$ , as published in Refs. [4, 5, 6, 7, 8, 9, 10, 11], and use the same inputs in the analysis of  $A_\perp$ ,  $F_1$  and  $R$  for all the data sets.

In the deep inelastic region the asymmetry  $A_\perp$ , or equivalently  $A_2 / \sqrt{2} = (1 + \cos^2 \theta) A_k + A_\perp$ , can be described by the (twist-2) Wandzura-Wilczek relation [17]. In the resonance region, however, this approximation fails, and here alternative parameterizations are required. A model-independent constraint on the size of  $A_2$  is provided by the Soer bound [18], although the available data [7] appear to be considerably lower than this limit. To provide a realistic description of  $A_2$  we combine the deep inelastic Wandzura-Wilczek contribution, including target mass corrections, with a model of the  $W < 2$  GeV region based on a constituent quark model [19] for the resonance part and a target mass corrected Wandzura-Wilczek term for the background.

For the ratio  $R(x; Q^2)$  we use a new parameterization [20, 21] based on Rosenbluth-separated cross sections, which is adapted to the low  $Q^2$  and large  $x$  region, and smoothly interpolates to the earlier parameterization of the deep inelastic region from Ref. [22]. This parameterization uses all published data in the resonance region [23], as well as preliminary data from Ref. [24].

The spin-averaged proton cross section is well determined in both the resonance and deep inelastic regions. While for the latter (at high  $Q^2$ ) the effect of  $R$  is small, and the differential cross section  $d^2 = d^2/dE^0$  is proportional to  $F_2$  (or  $F_1$ ), at moderate  $Q^2$  the extraction of  $F_1$  and  $F_2$  from the cross section requires knowledge of  $R$ . Using the parameterization of  $R$  from Ref. [20], we constructed a database of world data on  $F_1$  from which values of  $F_1$  corresponding to the measured  $A_k$  kinematic points were obtained by interpolation. Most of the points for  $A_k$  have kinematically close sets of  $d^2 = d^2/dE^0$  experimental points, thereby minimizing uncertainties due to interpolation. For instance, in the resonance region

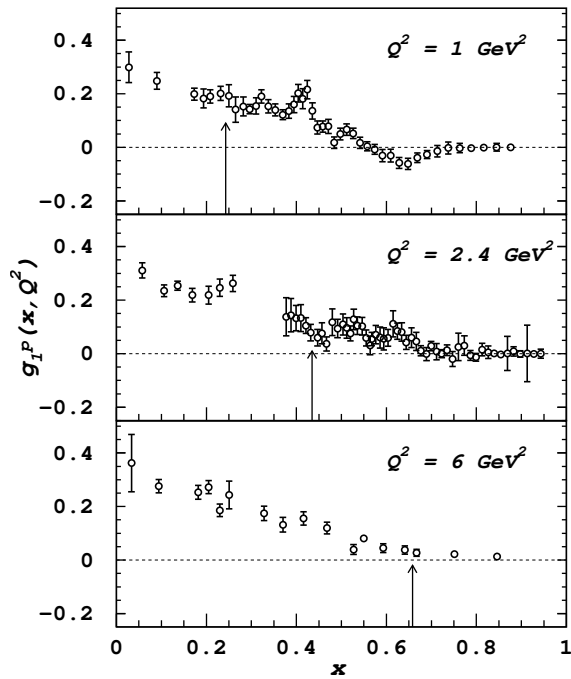


FIG. 1: Proton  $g_1$  structure function at several different  $Q^2$  values. The points represent reanalyzed experimental data obtained from the longitudinal asymmetry  $A_k$  from Refs. [4, 5, 6, 7, 8, 9, 10, 11] using the procedure described in the text. The vertical arrows indicate the boundary between the resonance (to the right of the arrow) and deep inelastic regions ( $W = 2 \text{ GeV}$ ).

the kinematics of the CLAS  $g_1$  experiment [11] is completely covered by the corresponding kinematic range of the  $d = d \text{ dE}^0$  measurements from Ref. [25]. Full details of the extraction of  $g_1$  will be provided in a forthcoming publication [21].

The resulting  $g_1$  structure function is illustrated in Fig. 1 as a function of  $x$  for several representative  $Q^2$  values. The vertical arrows indicate the boundary between the resonance and deep inelastic regions at  $W = 2 \text{ GeV}$ . At the lower  $Q^2$  values,  $Q^2 = 1 \text{ GeV}^2$ , a significant portion of the  $x$  range is in the resonance region (contributing 40% of the magnitude of the lowest moment).

The first moment of  $g_1$  is evaluated using the same method as in recent analyses of the unpolarized proton  $F_2$  structure function moments [25, 26]. This method is essentially independent of assumptions about the  $x$  dependence of the structure function when interpolating between data points, and is therefore well-suited for a study of  $Q^2$  evolution of the moments. For the low- $x$  extrapolation, beyond the region where data exist, we use the Regge model-inspired parameterization from Ref. [27]. To estimate the uncertainty associated with the low- $x$  extrapolation, we also consider several other parameterizations [28], and take the maximum difference between the respective low- $x$  contributions as the error.

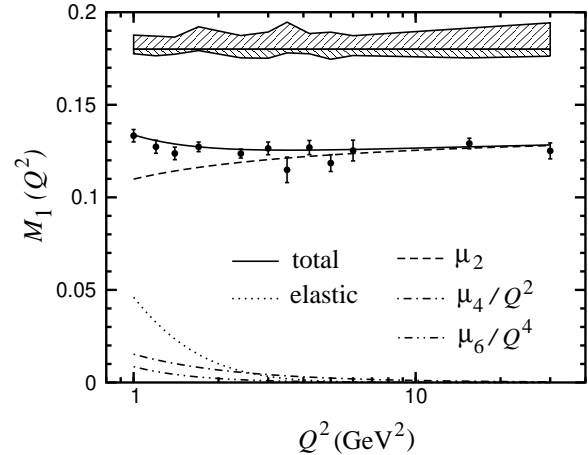


FIG. 2:  $Q^2$  dependence of the Nachtmann moment  $M_1(Q^2)$ . The error bars are statistical, with the systematic errors indicated by the hashed areas (see text). The leading twist (dashed),  $1=Q^2$  (dot-dashed),  $1=Q^4$  (dot-dot-dashed) and elastic (dotted) contributions are shown separately. The solid curve is the sum of leading and higher twist terms.

The resulting Nachtmann moment  $M_1(Q^2)$  is shown in Fig. 2, where the error bars on the data points are statistical only. The systematic errors, some of which are correlated, are shown separately in the hashed areas above the data, and include uncertainties from the low- $x$  extrapolation (lower hashed area), and from  $A_2, R$  and an estimated 5% uncertainty on the elastic contribution from the form factor parameterization of Ref. [29] (upper hashed area) to take into account the effect of the  $G_E^p = G_M^p$  suppression observed in recent experiments at Jefferson Lab [30]. The  $g_2$  contribution to  $M_1$  is obtained from  $A_k, A_2$ , and  $F_1$ , as determined from the present analysis (see Ref. [21] for details).

In fitting the total moment  $M_1(Q^2)$  we use three parameters,  $a_0^{\text{inv}}, f_2$  (or  $f_4$ ) and  $\mu_6$ , with the non-singlet axial charges ( $g_A$  and  $a_8$ ) as inputs. For the leading twist contribution we use a next-to-leading order approximation for the Wilson coefficients and the two-loop expression for  $\alpha_s$ , which at  $Q^2 = 1 \text{ GeV}^2$  corresponds to  $\alpha_s^{\text{NLO}} = 0.45 \pm 0.05$  in the  $\overline{\text{MS}}$  scheme. Assuming the data at high  $Q^2$  are saturated by the twist-2 term alone, the fit to the  $Q^2 > 5 \text{ GeV}^2$  data determines the singlet axial charge to be

$$a_0^{\text{inv}} = 0.145 \pm 0.018 \text{ (stat.)} \pm 0.103 \text{ (sys.)} \\ \pm 0.041 \text{ (low } x) \pm 0.006 \text{ (} \alpha_s \text{)} \pm 0.010 \text{ (} \alpha_s \text{)}; \quad (8)$$

where the first and second errors are statistical and systematic, the third is from the  $x \rightarrow 0$  extrapolation, and the last is due to the uncertainty in  $\alpha_s$ . The leading twist contribution to  $M_1$  is indicated by the dashed curve in Fig. 2.

Having determined the twist-2 term from the high  $Q^2$  data, we now extract the  $1=Q^2$  and the  $1=Q^4$  coefficients from the  $1=Q^2 \leq 5 \text{ GeV}^2$  data, fixing  $a_0^{\text{inv}}$  to the above value, but allowing it to vary within its statistical errors. For the twist-4 coefficient we find

$$f_2 = 0.039 \pm 0.022 \text{ (stat.)} \pm_{0.018}^{0.000} \text{ (sys.)} \\ 0.030 \text{ (low } x) \pm_{0.011}^{0.007} \text{ (} s \text{)} ; \quad (9)$$

normalized at a scale  $Q^2 = 1 \text{ GeV}^2$  (the  $Q^2$  evolution of  $f_2$  is implemented using the one-loop anomalous dimensions calculated in Refs. [31, 32]). The systematic uncertainty on  $f_2$  is determined by re fitting the  $M_1$  data shifted up or down by the  $M_1$  systematic uncertainty shown in Fig. 2 (upper hashed area). The low- $x$  extrapolation uncertainty is determined by fitting the  $M_1$  values shifted by the maximum difference between the  $x \rightarrow 0$  contributions calculated with the parameterizations from Refs. [27] and [28] (lower hashed area in Fig. 2).

For the  $1=Q^4$  term, the best fit to the  $1=Q^2 \leq 5 \text{ GeV}^2$  data yields  $f_6 = 0.011 \pm 0.013 \text{ (stat.)} \pm_{0.000}^{0.010} \text{ (sys.)} \pm_{0.011} \text{ (low } x) \pm_{0.000} \text{ (} s \text{)}$ , with the errors determined as for  $f_2$ . Within the present level of accuracy the  $Q^2$  evolution of the coefficient  $f_6$  can be neglected. The  $1=Q^2$  and  $1=Q^4$  contributions to  $M_1$  are illustrated in Fig. 2. For comparison, the elastic contribution is also shown, as is the sum of the leading plus higher twist contributions. Since one is fitting  $M_1$  in a relatively low  $Q^2$  region, one may ask whether still higher order corrections could be significant beyond those considered in Eq. (4). Adding a phenomenological  $1=Q^6$  term gives a coefficient  $f_8$  consistent with zero for  $Q^2 > 1 \text{ GeV}^2$ , with a large error. From this we conclude that an expansion up to  $O(1=Q^4)$  is sufficient to describe the data in this region.

In earlier phenomenological analyses [12, 13] larger values of  $f_2$  were obtained. Using the SLAC-E143 data [6], Ref. [12] found  $f_2 = 0.10 \pm 0.05$ , while Ref. [13] used in addition HERMES [10] and CLAS [11] data to extract a value  $f_2 = 0.15 \pm 0.18$ . In both cases the  $1=Q^4$  corrections in Eq. (4) were not included.

From the extracted  $f_2$  values one can calculate the contribution of the collective color electric and magnetic fields to the spin of the proton. Expressing the matrix elements in Eq. (6) in terms of the components of the dual field strength tensor in the proton rest frame, the color electric and magnetic polarizabilities of the proton can be defined as [33, 34]

$$E \cdot 2M^2 S = \langle N | \vec{j}_a \cdot \vec{E}_a | N \rangle ; \quad (10)$$

$$B \cdot 2M^2 S = \langle N | \vec{j}_a^0 \cdot \vec{B}_a | N \rangle ; \quad (11)$$

where  $\vec{E}_a$  and  $\vec{B}_a$  are the color electric and magnetic fields, respectively, and  $\vec{j}_a$  is the quark current. The

color polarizabilities can then be written as

$$E = \frac{2}{3} (2d_2 + f_2) ; \quad (12)$$

$$B = \frac{1}{3} (4d_2 - f_2) ; \quad (13)$$

where the coefficient  $d_2$  is given by the matrix element of the twist-3 operator  $(\mathcal{G} + \mathcal{G}^*)$ . The  $d_2$  matrix element can be extracted from the second moment of the  $g_1$  and  $g_2$  structure functions,

$$d_2(Q^2) = \int_0^1 dx x^2 [2g_1(x;Q^2) + 3g_2(x;Q^2)] ; \quad (14)$$

as determined from the present analysis. We find, however, that its leading twist component is negligible, and consistent with zero.

Combining the extracted  $f_2$  and  $d_2$  values obtained from the global analysis, we find

$$E = 0.026 \pm 0.015 \text{ (stat.)} \pm_{0.024}^{0.021} \text{ (sys.)} \quad (15)$$

$$B = 0.013 \pm 0.007 \text{ (stat.)} \pm_{0.012}^{0.010} \text{ (sys.)} \quad (16)$$

where the low- $x$  extrapolation and  $s$  uncertainties have been folded into the total systematic error. Since the color polarizabilities are dominated by  $f_2$ , the sign of the color electric polarizability is positive, while that of the color magnetic polarizability is negative. The upper limit on  $f_2$  in Eq. (9) thus yields non-zero values for  $E$  and  $B$ , while the lower limit gives values which are close to zero.

These results can be compared to model calculations. QCD sum rules generally predict negative values for the electric polarizabilities, and slightly positive values for the magnetic ones [35, 36],  $\sum \text{rule } E = 0.07$  and  $\sum \text{rule } B = 0.02$ . The MIT bag model on the other hand implies [14]  $E^{\text{bag}} = 0.10$  and  $B^{\text{bag}} = 0.06$ . Calculations based on the instanton vacuum model give [37]  $E^{\text{instanton}} = 0.03$  and  $B^{\text{instanton}} = 0.02$ . It is generally difficult to obtain reliable errors for model calculations given the ad hoc nature of some of the models. However, the large absolute values of  $E$  predicted in the sum rule and bag model calculations appear to be disfavored. The magnitude of the polarizabilities in the instanton model are consistent with our findings, but have the opposite sign.

More precise measurements of the structure functions at  $Q^2 \leq 1 \text{ GeV}^2$ , with smaller statistical and systematic errors, would reduce the uncertainty in the extracted higher twist coefficients, as would better knowledge of  $f_2$  at the relatively low  $Q^2$  values discussed here. The present findings suggest that higher twists are small and consistent with zero for  $Q^2 \leq 2 \text{ GeV}^2$ , thus confirming the validity of global duality for the proton  $g_1$  structure function in this region. Better determination of the  $g_2$  structure function at moderate and high  $Q^2$  is also vital

for the determination of the  $d_2$  matrix element, as well as of the  $g_1$  structure function itself. The uncertainty from the low- $x$  extrapolation would be significantly reduced by considering the isovector combination of  $g_1$  structure functions, as in the Bjorken sum rule. This can be done by combining the present results with neutron data obtained from  $^3\text{He}$  experiments, or from a combined proton and deuteron analysis. Data from CLAS at Jefferson Lab on the deuteron  $g_1$  structure function, as well as new data on the proton at higher  $Q^2$ , are currently being analyzed and should provide further insights into the nonperturbative structure of the nucleon.

We would like to thank G. Ricco for helpful contributions. This work was supported in part by the U.S. Department of Energy (DOE) contract DE-AC05-84ER40150, under which the Southeastern Universities Research Association (SURA) operates the Thomas Jefferson National Accelerator Facility (Jefferson Lab), and by DOE grants DE-FG02-96ER40960 (Old Dominion University) and DE-FG02-96ER41003 (College of William and Mary).

- 
- [1] M. Anselmino, B. L. Ioé and E. Leader, *Yad. Fiz.* 49, 214 (1989); V. D. Burkert and B. L. Ioé, *Phys. Lett. B* 296, 223 (1992); *J. Exp. Theor. Phys.* 78, 619 (1994); D. Drechsel, *Prog. Part. Nucl. Phys.* 34, 181 (1995).
- [2] I. Niculescu et al., *Phys. Rev. Lett.* 85, 1182, 1186 (2000).
- [3] A. De Rújula et al., *Annals Phys.* 103, 315 (1977).
- [4] M. J. A. Lguard et al., *Phys. Rev. Lett.* 37, 1261 (1976); *ibid.* 41, 70 (1978).
- [5] G. Baum et al., *Phys. Rev. Lett.* 45, 2000 (1980).
- [6] K. Abe et al., *Phys. Rev. D* 58, 112003 (1998).
- [7] P. L. Anthony et al., *Phys. Lett. B* 553, 18 (2003).
- [8] J. Ashman et al., *Nucl. Phys. B* 328, 1 (1989).
- [9] B. Adeva et al., *Phys. Rev. D* 58, 112001 (1998); B. Adeva et al., *Phys. Rev. D* 60, 072004 (1999); Erratum *-ibid.* D 62, 079902 (2000).
- [10] A. Arapetian et al., *Phys. Lett. B* 442, 484 (1998).
- [11] R. Fatemi et al., *Phys. Rev. Lett.* 91, 222002 (2003).
- [12] X. Ji and W. Melnitchouk, *Phys. Rev. D* 56, 1 (1997).
- [13] C. W. Kao et al., *Phys. Rev. D* 69, 056004 (2004).
- [14] X. Ji and P. Unrau, *Phys. Lett. B* 333, 228 (1994); X. Ji, *Phys. Lett. B* 309, 187 (1993).
- [15] S. A. Larin et al., *Phys. Lett. B* 404, 153 (1997).
- [16] O. Nachtmann, *Nucl. Phys. B* 63, 237 (1973).
- [17] S. Wandzura and F. W. Ilczek, *Phys. Lett. B* 72, 195 (1977).
- [18] J. Soer and O. V. Teryaev, *Phys. Lett. B* 490, 106 (2000).
- [19] M. Ferraris et al., *Phys. Lett. B* 364, 231 (1995).
- [20] M. E. Christy et al., in preparation.
- [21] M. O. Sitenko et al., in preparation.
- [22] K. Abe et al., *Phys. Lett. B* 452, 194 (1999).
- [23] J. Drees et al., *Z. Phys. C* 7, 183 (1981); K. Batzner, Ph.D. thesis (1972); D. Baran et al., *Phys. Rev. Lett.* 61, 400 (1988).
- [24] C. Keppel, Jefferson Lab experiment E94-110.
- [25] M. O. Sitenko et al., *Phys. Rev. D* 67, 092001 (2003).
- [26] C. S. Amstrong et al., *Phys. Rev. D* 63, 094008 (2001).
- [27] S. Simula et al., *Phys. Rev. D* 65, 034017 (2002).
- [28] M. Glück et al., *Phys. Rev. D* 63, 094005 (2001); D. de Florian and R. Sassot, *ibid.* D 62, 094025 (2000).
- [29] P. Mergell et al., *Nucl. Phys. A* 596, 367 (1996).
- [30] M. K. Jones et al., *Phys. Rev. Lett.* 84, 1398 (2000); O. Gayou et al., *Phys. Rev. Lett.* 88, 092301 (2002).
- [31] E. V. Shuryak and A. I. Vainshtein, *Nucl. Phys. B* 201, 141 (1982).
- [32] H. Kawamura et al., *Mod. Phys. Lett. A* 12, 135 (1997).
- [33] E. Stein et al., *Phys. Lett. B* 353, 107 (1995).
- [34] X. Ji, in Proceedings of the 7th International Conference on the Structure of Baryons, Santa Fe, New Mexico (1995), hep-ph/9510362.
- [35] I. I. Balitsky, V. M. Braun and A. V. Kolesnichenko, *JETP Lett.* 50, 61 (1989); *Phys. Lett. B* 242, 245 (1990); Erratum *-ibid.* B 318, 648 (1993).
- [36] E. Stein et al., *Phys. Lett. B* 343, 369 (1995).
- [37] N. Y. Lee et al., *Phys. Rev. D* 65, 054008 (2002).